Macromolecules **1994,** *27,* 989–996

Crystal Structure, Morphology, and Phase Transitions in Aromatic Polyimide Oligomers. 1. Poly(4,4′-oxydiphenylene pyromellitimide)

Jiang Liu, Stephen Z. D. Cheng,* and Frank W. Harris

Institute and Department of Polymer Science, College of Polymer Science and Polymer Engineering, The University of Akron, Akron, Ohio 44325-3909

Benjamin S. Hsiao and Kenncorwin H. Gardner

Fiber and Central Research and Development Department Division, Experimental Station, E. I. du Pont de Nemours and Company, Wilmington, Delaware 19880

Received August 23, 1993; Revised Manuscript Received November 12, 1993●

ABSTRACT: The crystal structure and morphology of a polyimide oligomer synthesized from pyromellitic dianhydride (PMDA) and 4,4′-oxydianiline (ODA) in the melt state have been studied via transmission electron microscopy (TEM), electron diffraction (ED), and wide-angle X-ray diffraction (WAXD). The unit cell of PMDA–ODA was found to crystallize in a two-chain orthorhombic unit cell with dimensions a = 0.836 nm, b = 0.563 nm, and c = 3.303 nm. This unit cell is different from those cells previously reported for PMDA–ODA fibers or oriented films prepared by an imidization process from poly(amic acid) precursors and annealed at elevated temperatures. However, this unit cell compares well to those of aromatic polyimides based on PMDA and similar diamines. This cell can only be observed at relatively low temperatures. Prolonged annealing at elevated temperature (above 300 °C) always leads to a transformation of this low-temperature orthorhombic unit cell I to a high-temperature orthorhombic unit cell II which is close to those previously reported. This irreversible transformation was also confirmed by differential scanning calorimetry (DSC) experiments. The observed crystal morphology is primarily lamellar with extended-chain conformations. The thickness of the lamellar crystal varies with the polymerization conditions. In addition to the normal single lamellar crystal, twined lamellar crystals with an angle of 69° between the two a-axes are most frequently observed. Other twin crystals with angles of 38° and 25° are also found, but less frequently. Possible lattice packing relationships in these twin crystals are discussed. In addition, lamellar crystals with an angle of 90° between the two a-axes are observed, which is indicative of the epitaxy growth on the crystalline planes (100) and (010).

Introduction

Crystallization during polymerization often results in large single crystals with little chain folding and few internal defects. This phenomenon is a distinct branch in the polymer crystal and crystallization study, apart from the more common melt and solution methods of growing macromolecular crystals. The earliest examples of crystals grown during polymerization was poly(oxymethylene) made from a concentrated formaldehyde solution by the addition of concentrated sulfuric acid. Hexagonal prisms of perfect poly(oxymethylene) morphology with a size of 0.05 mm were shown by Staudinger and Signer as early as 1929.[1,2] The molecular chain axis was shown to be parallel to the prism axis so that with sufficiently high molecular weight a perfect crystal should result. An early review of this topic appeared in 1968[3] where a large list of inorganic polymer single crystals derived during polymerization has been summarized. During the polymerization, monomers are either in the gas, solution, or melt state to carry out crystallization by depositing onto the crystal surfaces, where the polymerization takes place simultaneously. In most cases, the nucleation steps cannot be fully investigated since the subsequent crystallization is too complicated.

If the polymerization is carried out in the melt, the product is usually a solid, crystalline polymer. Many examples can be found in the literature such as polyolefins, poly(oxymethylene), some polyamides, and selenium.[4] Very recently, this method has also been adopted to study the structure and crystallization of a series of liquid crystalline polyesters and copolyesters.[5,6] Lamellar morphologies with the chain axis aligned perpendicular to the lamellar surface have been reported in almost every case.

Aromatic polyimides have been a class of materials which possess a combination of excellent macroscopic properties such as high thermal and thermooxidative stability, good mechanical properties, chemical resistance, low dielectric constant, and, sometimes, outstanding optical properties. The most widely studied polyimide to date is poly(4,4′-oxydiphenylene pyromellitimide) synthesized from pyromellitic dianhydride (PMDA) and 4,4′-oxydianiline (ODA) through a two-stage polymerization method. Basically, soluble poly(amic acid) precursors are first polymerized in *N*-methyl-2-pyrrolidone (NMP), and then, the poly(amic acid)s are imidized by a thermal or a chemical route.[7] This polymer has been commercially available under the trade name of Kapton by DuPont.[8,9]

An earlier study of PMDA–ODA fibers by wide-angle X-ray diffraction (WAXD) showed that the unit cell of PMDA–ODA is orthorhombic with a = 0.631 nm, b = 0.397 nm, and c = 3.20 nm (in order to fit the common custom in crystallographic study, the longer length in the unit cell is assigned to be a-axis).[10,11] The chain was determined to be in a 2_1 helical conformation along the c-axis, and the one-chain per unit cell packing was determined. Others also reported a monoclinic unit cell with a = 0.59 nm, b = 0.46 nm, c = 3.29 nm, and γ = 100°.[12] Recently, the orthorhombic PMDA–ODA unit cell has been confirmed but with slightly different cell dimensions: a = 0.646 nm, b = 0.403 nm, and c = 3.26 nm by Gardner using WAXD of fibers and highly oriented films.[13] The differences between these PMDA–ODA unit cell lattices and dimen-

---

* To whom the correspondence should be addressed.

● Abstract published in *Advance ACS Abstracts,* January 1, 1994.

0024-9297/94/2227-0989$04.50/0

sions may result from different imidization processes and the degree of imidization. The crystal morphology of PMDA–ODA has not been extensively reported due to a difficulty of controlling the imidization process. Recently, PMDA–ODA crystal lattice images have been obtained by Martin using high-resolution transmission electron microscopy (TEM) and atomic force microscopy.[14] Lattice defects were found in the PMDA–ODA orthorhombic lattice with the angle γ around 81–99°. Therefore, the obtained lattice should be more precisely termed "pseudoorthorhombic". Computer modeling work to simulate the crystal unit cell has resulted in an orthorhombic cell with $a = 1.32$ nm, $b = 0.386$ nm, and $c = 3.28$ nm.[15]

In this paper, we report out attempt to obtain single lamellar crystals of PMDA–ODA oligomers by crystallization during polymerization in the melt state. A new orthorhombic unit cell has been observed in the as-polymerized crystals by electron diffraction (ED) and confirmed by WAXD. This unit cell contains two chains. Twin crystals and epitaxy crystal growth have been observed via TEM and ED. Their lattice packing relations are also discussed. It is further found that this new unit cell (cell I) is only stable at relatively low temperatures. Prolonged annealing at elevated temperatures (say, above 300 °C for several hours) leads to a transformation of this cell I into a high-temperature orthorhombic unit cell II, which possesses the unit cell dimensions which are close to those previously reported.[10–13]

Experimental Section

Materials. Pyromellitic dianhydride (PMDA) and 4,4′-oxydianiline (ODA) monomers were purchased from Chriskev Inc. These monomers were characterized by differential scanning calorimetry (DSC; Seiko DSC-220) at a 10 °C/min heating rate. The melting temperature for PMDA is 286 °C and that for ODA is 192 °C (the width of half-height of a few degrees). The monomers were separately dissolved in acetone with equal molar concentrations of about 0.5% at room temperature. Using a method similar to that developed by Geil and co-workers,[5,6] thin films of polyimide crystals were prepared by one-step and two-step methods. In the one-step method, equal molar ratios of PMDA and ODA solutions were cast onto separate clean glass slides to obtain an appropriate stoichiometry and were allowed to dry. The glass slides were then placed together to make close contact with each other. Condensation polymerization and imidization were allowed to take place simultaneously by subsequent heating. In the two-step method, the two monomer solutions with equal molar ratios were mixed first, cast as thin films on one glass slide, and allowed to dry. The condensation polymerization occurred before drying within a few seconds. A clean glass slide was used as a cover after the drying. Further condensation and imidization progressed simultaneously at elevated temperatures.

The sandwiched slides obtained from both methods were wrapped in an aluminum foil and heated to various predetermined temperatures and times under dry nitrogen in an oven (Isotemp Vacuum Oven, Model 282 A). After polymerization, the recovered materials were heated up to even higher temperatures under vacuum to complete the imidization and eliminate H_2O off gas and residual monomers. The high-temperature-treated polyimide specimens were then separated and washed three times in boiling acetone and tetrahydrofuran (THF). For molecular weight and molecular weight distribution determination, the melt-polymerized samples were first dissolved in pentafluorophenol (80 °C) and then transferred to a high-temperature GPC apparatus (Water 150C) using mixed solvents of trichlorobenzene and phenol (50:50) at 115 °C. The GPC apparatus was calibrated by polystyrene standards. The number-average molecular weight was estimated to be about 2000 with a polydispersity of 2.5. The molecular weight over 10 000 is about 10% of the sample. The intrinsic viscosity is 0.22 in the mixed solvent. A minor increase of the molecular weight was found (less than 20%) after the samples were annealed between 300 and 400 °C for 1 h.

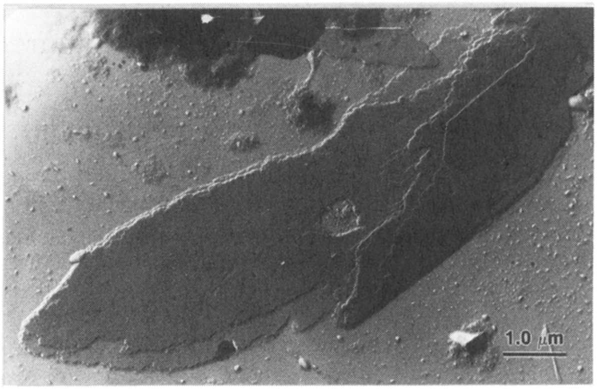

Figure 1. PMDA–ODA lamellar crystal morphology observed in TEM.

Instrumentation and Experiments. The nascent polyimide films (thickness of about 0.1 μm) from the glass slides were examined by transmission electron microscopy (TEM; JEOL 1200EX II at 120 kV) and electron diffraction (ED). The thin films were first shadowed with Pt–C and coated with carbon, retrieved from the glass slides by using poly(acrylic acid) films, and then floated on water and picked up on TEM grids. Calibration of the electron diffraction spacings was carried out using Au and TlCl (d spacing < 0.384 nm, the largest spacing for TlCl). Spacing values larger than 0.384 nm were calibrated by doubling the d spacings of those reflections of the polymer based on the spacing of its first-order reflection. Low-beam dosage techniques were used, and the ED patterns obtained from the polyimide films were considerably more stable in radiation than polyethylene and poly(ethylene oxide) single crystals.[16] In order to determine the three-dimensional crystal lattice, a tilting angle stage in TEM was used to examine ED patterns.

Wide-angle X-ray diffraction (WAXD) experiments were conducted using a Rigaku 12-kW rotating-anode generator coupled with a diffractometer. The monochromatized X-ray beam consisting of Cu Kα with a wavelength of 0.154 nm was used for this measurement. The PMDA–ODA oligomer powder samples were annealed at different temperatures between 300 and 400 °C for 1 h and then quenched to room temperature. The WAXD experiments were performed in $2\theta = 1.8$–35°. To study the anisotropic structure of the PMDA–ODA oligomer films polymerized on the glass slides, a reflection mode of WAXD was used. This is because, if the chain molecular direction is perpendicular to the glass slide surface, the reflection WAXD pattern should represent the (00l) crystalline planes of the PMDA–ODA crystals.

Differential scanning calorimetry (DSC) measurements were conducted via a Seiko DSC 220. The samples (about 10 mg) were directly annealed in DSC at temperatures varying from those for WAXD experiments and then cooled to 200 °C. The subsequent heating traces were recorded at 10 °C/min to 500 °C. The DSC was calibrated using the standard procedure.

The density measurements of the samples were carried out in a density gradient column using a hexane–carbon tetrachloride system at 25 °C.

Results and Discussion

New Unit Cell I Determination. We found that crystallization during polymerization avoided long-chain crystallization kinetics effects and provided well-defined single lamellar crystals with high crystallinity, better crystal packing, and extended-chain conformation. Figure 1 shows a typical TEM micrograph of PMDA–ODA crystals after the two-step polymerization (260 °C for 1 h), followed by annealing at 300 °C for 1 h in vacuum. The crystals are lamellar having different thickness. Most of lamellae are not faceted with relatively irregular shapes along the edges but possess a very smooth top surface. Figure 2a is an ED pattern taken from Figure 1. This pattern exhibits sharp diffractions ($hk0$ reflections) that

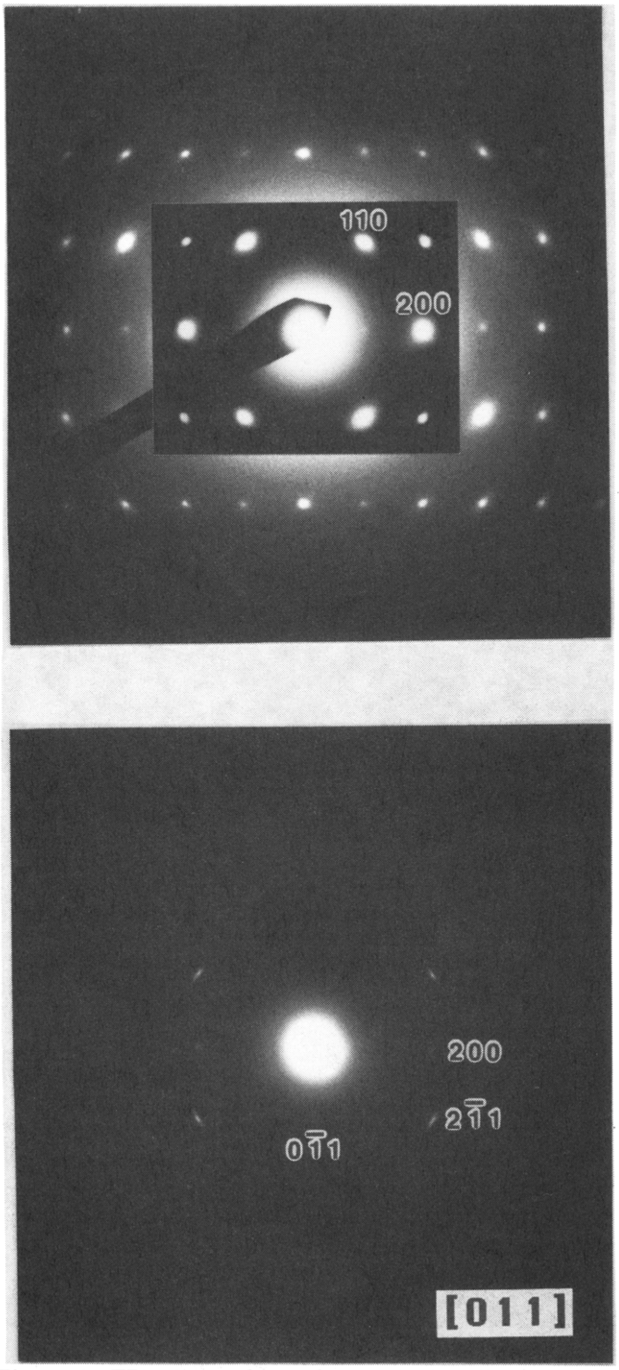

Figure 2. ED pattern obtained from the lamellar crystals in Figure 1. The chain direction is perpendicular to the basal plane (a) and a tilted ED pattern of the crystals in Figure 1 at an angle of 15° about the *a*-axis (b).

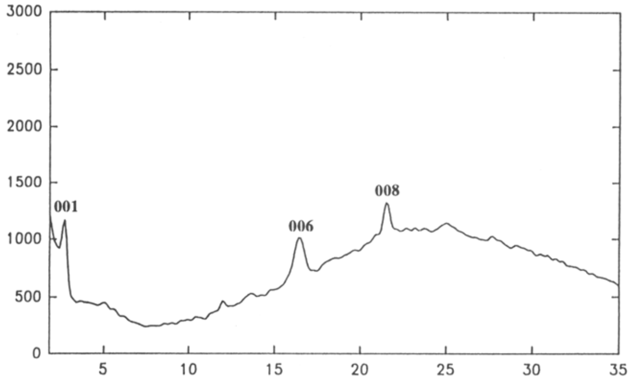

Figure 3. WAXD pattern of a thin film sample with a glass slide substrate in the reflection mode. Note that only (00*l*) crystalline reflections are observed.

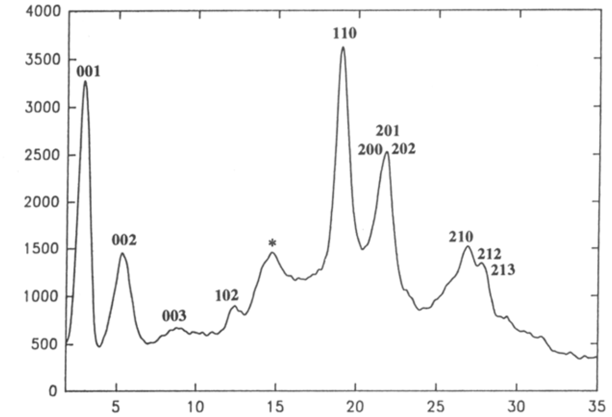

Figure 4. WAXD pattern of PMDA–ODA powder samples. The assignments are based on the unit cell I dimensions determined from ED. Note the peak marked with an asterisk cannot be assigned.

have been interpreted as the a^*b^* plane with the c-axis perpendicular to the basal plane (substrate). To determine the unit cell dimension along the c-axis, a series of ED patterns were collected using a tilting angle stage. The ED pattern obtained by a tilt angle of 15° about the a-axis is shown in Figure 2b. The (*hkl*) reflections observed in this and other tilted patterns allowed the three-dimensional reciprocal lattice to be defined. The ED patterns were indexed by a two-chain orthorhombic unit cell with dimensions $a = 0.836$ nm, $b = 0.563$ nm, and $c = 3.303$ nm. The crystalline density is calculated to be 1.63 g/cm^3 which compares with the measured PMDA–ODA density of 1.58 g/cm^3. This new unit cell parameter is different from those previously reported in studies of highly oriented fibers or films (Table 1[10–13,17]). These other samples were obtained from isolated poly(amic acid)s and subsequently imidized through a thermal or a chemical method,[7] followed by annealing at elevated temperatures to develop maximum crystallinities. Consequently, the different thermal and chemical histories might have led to varying degrees of imidization and crystallinity as well as different chain packing. The new unit cell I parameters determined here are very different (both dimensions and symmetry) from the earlier PMDA–ODA unit cells. This difference is beyond the expectation of polymerization and imidization effects and thus is attributed to a new unit cell lattice (cell I) as a polymorph in PMDA–ODA crystals. The previously reported orthorhombic unit cell[10,11,13] is thus referred to as cell II. The morphologies obtained from both polymerization methods (one-step and two-step methods) are similar, and the ED patterns are the same.[18]

The chain direction in lamellar crystals is also examined through WAXD experiments in reflection mode. In this case, the WAXD pattern should only exhibit (00*l*) crystalline diffractions if chain molecules are perpendicular to the substrate surface. This is shown in Figure 3 where all diffraction peaks can be indexed by (00*l*) reflections in cell I. We have also carried out the PMDA–ODA oligomer powder WAXD experiments (results shown in Figure 4) and found that the diffraction pattern corresponds well to the unit cell parameters determined from ED (Figure 2). In Figure 4, the WAXD powder pattern of PMDA–ODA is in general agreement with the cell I structure (selected assignments of the reflection peaks are included here); however, the peak at around $2\theta = 14.6°$ (peak marked with an asterisk in the figure) with a relatively weak intensity cannot be assigned based on the cell I parameters.

Table 1. Comparison of Lattice Parameters of PMDA-Based Aromatic Polyimides

repeat unit of polyimide	a (Å)	b (Å)	c (Å)	α, β, γ	no. of chains per cell
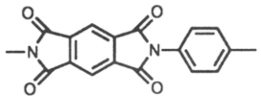	8.5	5.6	12.3	90	2
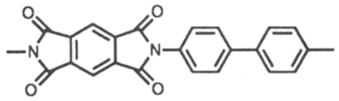	8.4	5.6	16.6	90	2
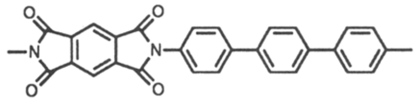	8.4	5.5	20.9	90	2
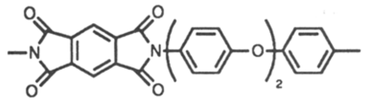	8.3	5.65	21.9	90[a]	2
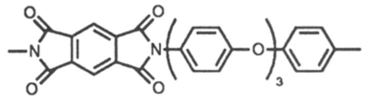	8.4	5.65	53.3	90	2
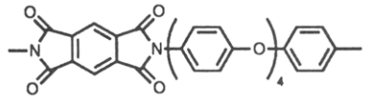	8.35	5.6	30.1	90	2
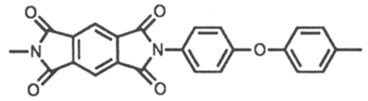	6.3	4.0	32.0	90	1
	5.9	4.6	32.9	90, 90, 100	1
	6.46	4.03	32.58	90	1
	13.2	3.86	32.8	90	2
cell I	8.36	5.63	33.03	90	2
cell II	5.93	4.70	33.00	90	1

[a] Some reports determined as a monoclinic lattice.

This odd peak will be explained in the later part of this paper.

Further insight into the PMDA–ODA cell I can be gained by comparing it with the unit cells of PMDA-based polyimides containing structurally similar diamines (Table 1). With the exception of the reported structures of PMDA–ODA (cell II), polymers prepared by polymerizing PMDA with diamines containing just phenyl or phenyl and ether moieties crystallize in two-chain orthorhombic unit cells with similar ab projections (a = 0.83–0.85 nm, b = 0.55–0.565 nm). The c-axes of these polyimides are determined by the size and complexity of the diamines. The PMDA–ODA cell I (a = 0.836 nm, b = 0.563 nm) is consistent with these other two-chain crystal structures. The PMDA–ODA cell II, observed in fibers or films, is the only one-chain unit cell in this family of polyimides.

In micrographs like that shown in Figure 1, the difference between the thicknesses of two neighboring lamellae is always 6.6 nm, which corresponds to two c-axis repeats or four chemical moieties. The reason for this observation is not yet understood, but we speculate that this may be associated with paths of polymerization and crystallization processes of PMDA–ODA from the melt. At the thicker region of the lamellar crystals, we estimate that the chain length should be over 70 nm. The ED pattern taken from the thick lamellae (thicknesses greater than 70 nm) shows virtually the same as those taken from the thin film crystals (Figure 2) with a slightly different broadness of the (00l) diffraction lattice spots. A (200) reflection used in dark field imaging and its corresponding bright field TEM micrographs is shown in parts a and b of Figure 5, respectively. The crystal thickness is over 50 nm. Some regions do show Moire patterns, which indicates that the film most likely consists of several layers of extended chains with only a few degrees of rotation between the lamellae.

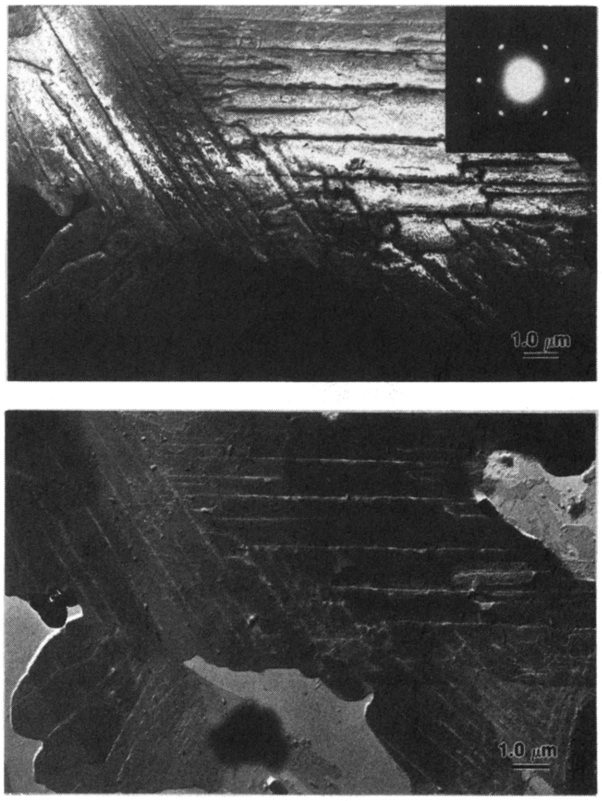

Figure 5. Pair of dark field (a) and corresponding bright field (b) TEM photographs of a thick PMDA–ODA lamellar crystal sample.

Twin Crystals and Epitaxy Growth. Figures 6–8 show a series of TEM micrographs with PMDA–ODA oligomer lamellar crystals exhibiting two different growth

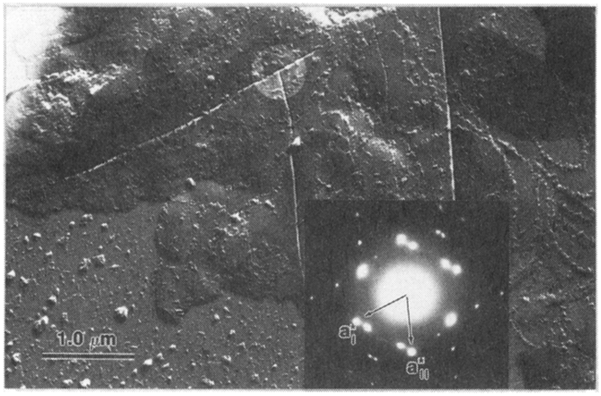

Figure 6. Twin crystal morphology with an angle of 69° between two *a*-axes observed in TEM and ED.

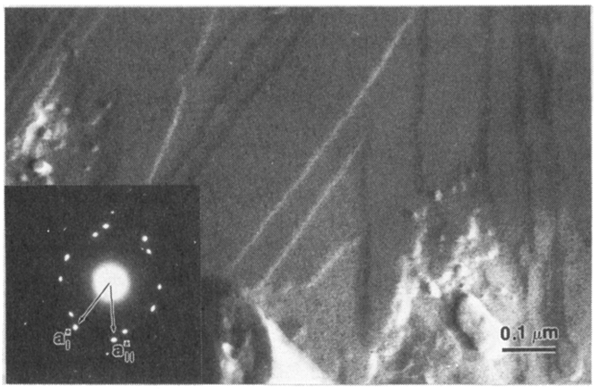

Figure 7. Twin crystal morphology with an angle of 38° between two *a*-axes observed in TEM and ED.

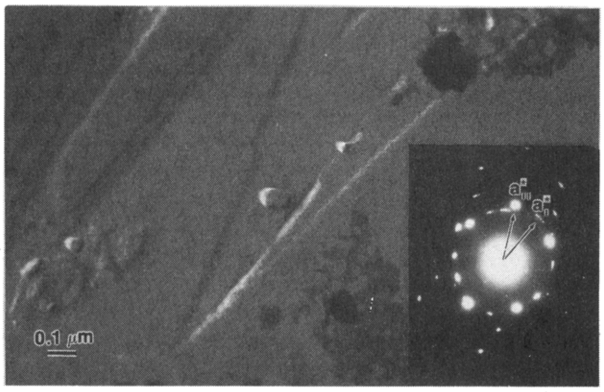

Figure 8. Twin crystal morphology with an angle of 25° between two *a*-axes observed in TEM and ED.

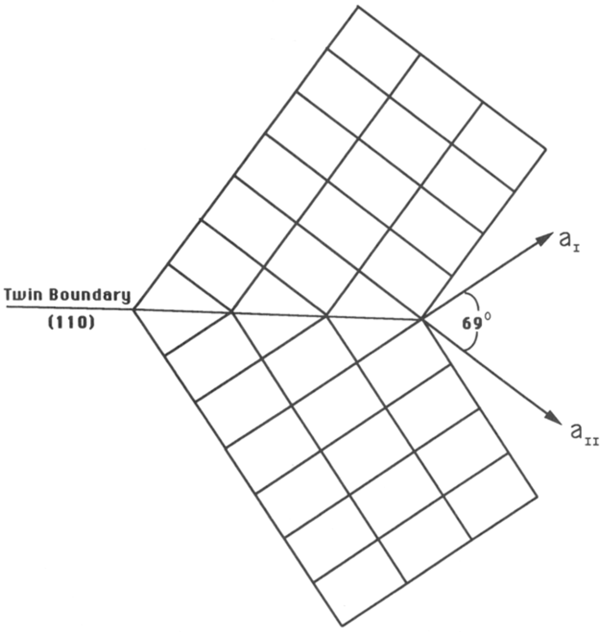

Figure 9. Twin crystal packing illustration as shown in Figure 6.

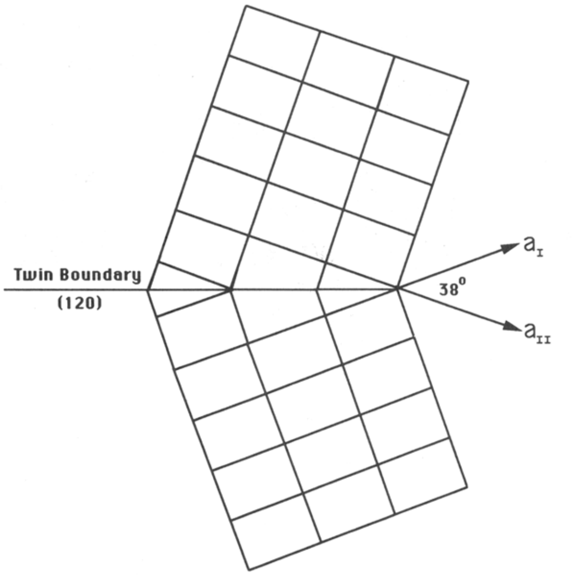

Figure 10. Twin crystal packing illustration as shown in Figure 7.

directions and symmetry. In Figure 6, the ED pattern indicates that the two *a*-axes (the same direction as the *a**-axis in the reciprocal lattice) show a crystallographic mismatch of 69°, and these unit cells with two different *a*-axes are derived from one single lamellar crystal. Therefore, this phenomenon indicates the presence of a twin crystal. This is because a twin crystal can consist of two lamellae joined macroscopically in a symmetrical fashion to form a single entity and contains an added element of macroscopic symmetry (along the twin boundary) over and above that which either component possesses. The observed twin crystal with an angle of 69° between the two *a*-axes is by far the major population observed in PMDA–ODA lamellar morphology. Other types of twin crystals have also been found, as shown in Figures 7 and 8. In these twin crystals the two *a*-axes are separated by angles of 38° and 25°, respectively, as seen by the corresponding ED patterns. A detailed crystallographic analysis indicates that these twin crystals possess twin boundaries of (110)–($1\bar{1}0$) (69°), (120)–($1\bar{2}0$) (38°), and (130)–($1\bar{3}0$) (25°), respectively. They are illustrated in Figures 9–11. An additional symmetry in the lamellar crystals can thus be found due to the presence of each twin boundary. It is clear that formation of the (110)–($1\bar{1}0$) twin boundary introduces the least amount of defects in the crystals. Therefore, this morphology becomes the major population in TEM observation compared with the other two twin crystals.

On the other hand, Figure 12 shows a 90° mismatch between the two *a*-axes in a PMDA–ODA lamellar crystal (Figure 12). This indicates that the (100) crystalline plane has to match the (010) plane in the crystal. The concept of a twin crystal cannot be utilized here since no additional symmetry is provided (note that the ratio of the *a*- and *b*-axes is not integral in this case). Epitaxy crystal growth is thus invoked. Figure 13 manifests the crystal packing of these two crystalline planes as the two *a*-axes are perpendicular to each other. It is obvious that the length of every two unit cells along the *a*-axis matches that of

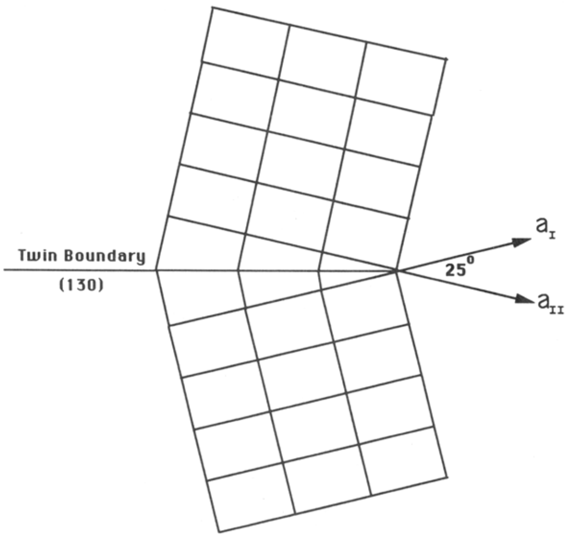

Figure 11. Twin crystal packing illustration as shown in Figure 8.

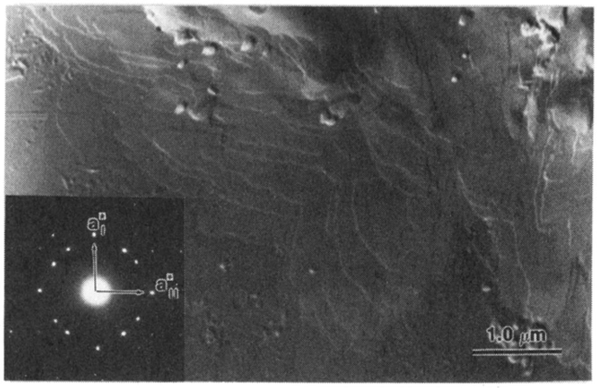

Figure 12. Epitaxy crystal growth with an angle of 90° between two *a*-axes observed in TEM and ED.

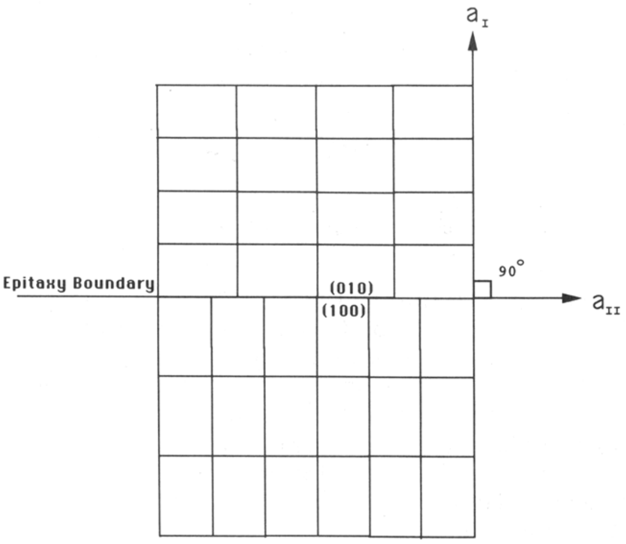

Figure 13. Epitaxy crystal packing illustration as shown in Figure 12.

three unit cells along the *b*-axis. In this case, some defects have to be introduced in order to satisfy the epitaxy growth pattern. Detailed analysis for the chain packing in both twin crystals and epitaxy growth will be the subject of a future study.

Transformation from the Low-Temperature Cell I to High-Temperature Cell II. A surprising observation was made from DSC heating experiments of a PMDA–ODA oligomer sample polymerized at 200 °C (1 h; one-step method) and further annealed at different temperatures (Figure 14). At an annealing temperature of 300 °C, a clear first-order endothermic transition peak is found at 366 °C, with a heat of fusion of 11.6 kJ/mol. When the annealing temperature increases from 300 to 360 °C, it is seen that this endotherm increases its peak temperature but decreases its heat of fusion (Figure 14). At an annealing temperature of 360 °C, no endothermic peak can be found. The DSC results indicate that a phase transformation

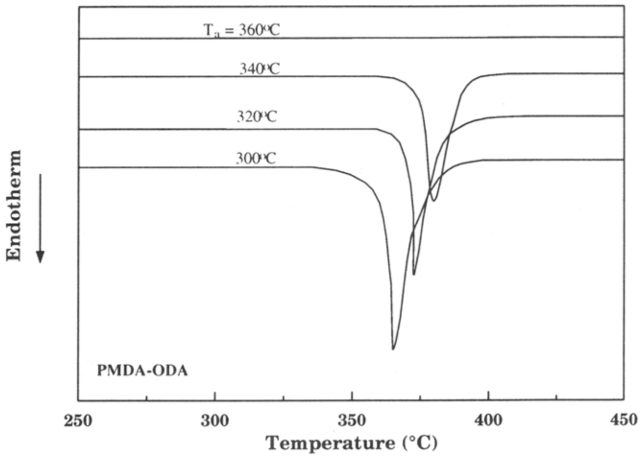

Figure 14. Set of DSC thermograms during heating for PMDA–ODA crystals annealed at different temperatures for 1 h.

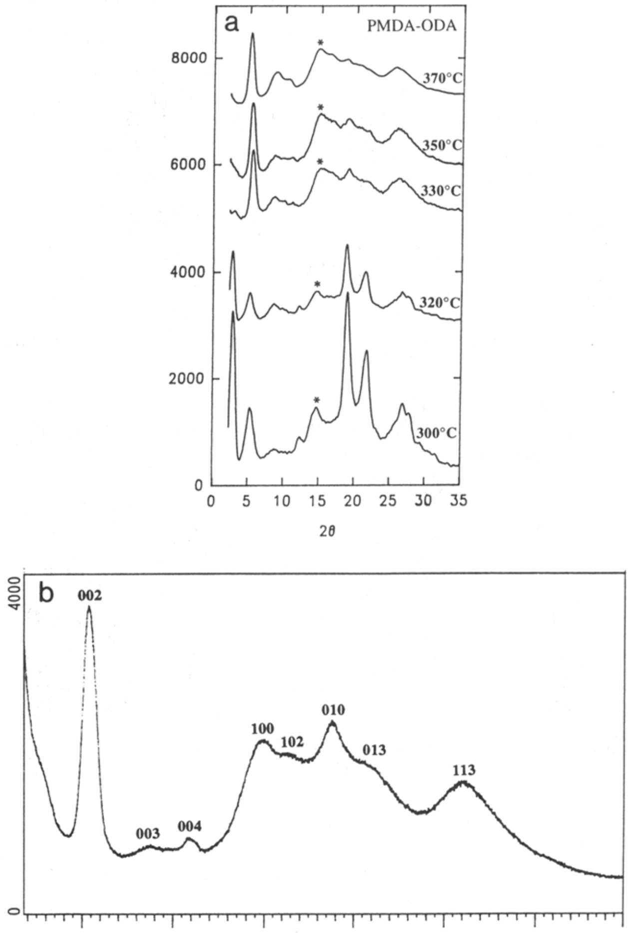

Figure 15. Set of WAXD powder patterns for PMDA–ODA crystals annealed at different temperatures for 1 h (a) and a WAXD pattern for PMDA–ODA crystals directly obtained through polymerization at 320 °C for 3 h (b).

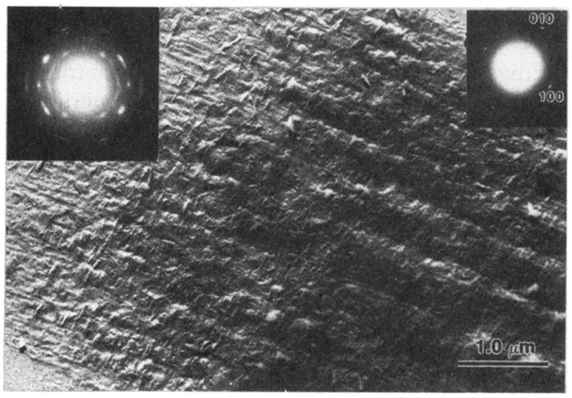

Figure 16. TEM and ED observations of the PMDA–ODA crystals after annealing at 400 °C for 10 min.

probably occurs during the annealing, and this transformation is irreversible upon cooling. A corresponding study of powder samples of WAXD annealed at different temperatures for 1 h is shown in Figure 15a. The low-temperature patterns, characteristic of cell I, are different from the high-temperature patterns, indicating a transformation from one crystalline phase to another. We have examined the WAXD powder pattern of the PMDA–ODA crystals after being annealed at 370 °C for 1 h. The diffraction peaks correspond well to the WAXD pattern reported by Gardner[13] and Ikeda.[19] In fact, the unassigned diffraction peak at $2\theta = 14.6°$ in Figure 4 can be attributed to the diffraction of (100) in cell II. This reveals that even the PMDA–ODA crystal annealed at 300 °C for 1 h has shown an initial structural transformation to cell II. Mixtures of both cells can be observed in Figure 15 for the samples annealed at temperatures between 300 and 370 °C. It is noticed that the intensities of (110) and (200) crystalline planes in cell I gradually decrease and, finally, almost vanish. The alternating changes of the intensities of (001) and (002) crystalline planes in the low-angle region are also surprising since the *c*-axis is not changed in both cells. This must be due to a dramatic rearrangement of the chain conformation and packing. The structure of cell II can also be directly obtained through polymerization at high temperatures for prolonged times, as shown in Figure 15b.

Figure 16 shows crystal morphology and ED patterns of PMDA–ODA crystals after annealing at 400 °C for 10 min. The surface appearance of lamellae becomes rough, but the chains remain perpendicular to the lamellar crystal surface as indicated by the ED patterns. On the basis of the WAXD and ED patterns (Figures 15 and 16), an orthorhombic unit cell dimension can be determined with $a = 0.593$ nm, $b = 0.470$ nm, and $c = 3.300$ nm. This unit cell II is close to the unit cells determined previously[10-13] and indicates that the cell II is a polymorph of PMDA–ODA crystals stabilized at high temperatures. The calculated crystallographic density is 1.38 g/cm^3, and the measured density of the samples is 1.34 g/cm^3. In Figure 16, and ED pattern at the upper-right corner indicates clearly the reciprocal lattice of cell II in the $[00l]$ zone (the *c*-axis perpendicular to the substrate), while that at the upper-left corner of Figure 16 shows a twin crystal in this crystal form with a (210)–$(2\bar{1}0)$ twin boundary (113° between two *a*-axes) as illustrated by an ED pattern shown in Figure 17a. Figure 17b is a scheme of the twin crystal packing based on the cell II.

The reason why the low-temperature orthorhombic unit cell (cell I) has never been observed before can be addressed as follows. In the past all PMDA–ODA fiber patterns were obtained through prolonged high-temperature treatment in order to achieve complete imidization and high crystallinity/orientation. Such annealing processes lead to a transformation of cell I to cell II. If one compares the difference in dimensions between these two cells, the *b*-axis in cell I is smaller than the *a*-axis in cell II by a distance of 0.03 nm, while the *a*-axis in cell I is almost double the *b*-axis in cell II (a 0.104-nm difference is seen). As a result, the overall expansion of the cross section of the unit cell along the *ab* plane (an expansion of 0.086 nm^2 from cell I to cell II) may satisfy the requirement of the phase transformation. One of the most important features of the WAXD patterns for cell I is the strong $(00l)$ reflection (Figure 3), and this is systematically absent in cell II (Figure 15). This illustrates that the phase transformation may

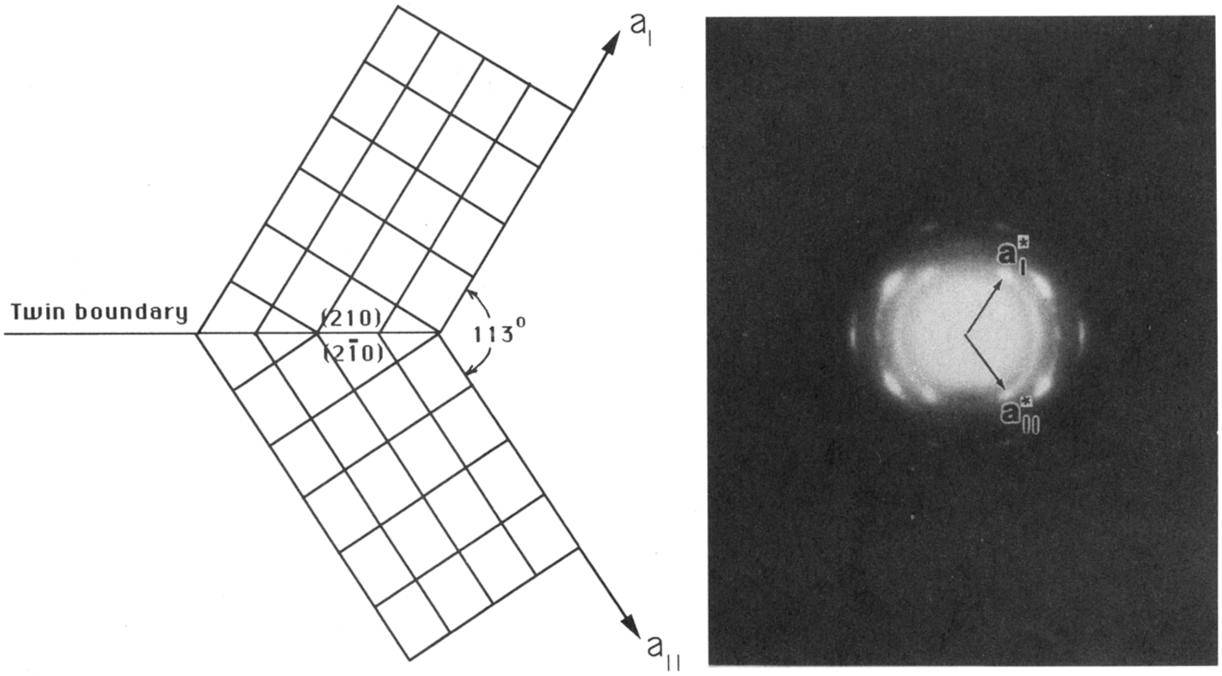

(b) (a)

Figure 17. ED of the twin crystal with an angle of 113° between two *a*-axes (a); twin crystal packing (b).

be accompanied by a chain conformation change and, therefore, a chain packing change. However, detailed changes are still not known at this moment.

Finally, it is also interesting to note some special features of the polymerization carried out in the melt. First, the poly(amic acid) precursors in this reaction are not isolated. When the reaction temperature is above both the melting temperatures of dianhydride and diamine, the reaction is carried out in the melt state; while the temperature is in between the melting temperatures of these two monomers, the reaction takes place on the surface of dianhydrides as an interfacial polymerization. Second, this kind of polymerization usually results in low molecular weight oligomers due to the limited melt flow. This leads to the growth of relatively large single lamellar crystals, which provides a necessary condition for the study of PMDA–ODA crystal structure and morphology via TEM and ED experiments. However, it is expected that the existence of the new PMDA–ODA crystal form (cell I) should be independent of the preparation methods of this polyimide.

Conclusion

We have reported a new two-chain orthorhombic unit cell (cell I) with $a = 0.836$ nm, $b = 0.563$ nm, and $c = 3.303$ nm for PMDA–ODA crystals directly synthesized from the melt state, based on their ED and WAXD observations. Lamellar crystals are observed with extended-chain conformations. The c-axis is perpendicular to the lamellar surface as well as the substrate surface. In addition to the normal unfaceted lamellar crystals, twin crystals are found with (110)–(1$\bar{1}$0), (120)–(1$\bar{2}$0), and (130)–(1$\bar{3}$0) twin boundaries. Among them, the twin crystal with a (110)–(1$\bar{1}$0) boundary is most frequently observed. Epitaxy growth between (100) and (010) crystalline planes is also seen. Cell I transforms to a high-temperature, one-chain orthorhombic unit cell (cell II) with $a = 0.593$ nm, $b = 0.470$ nm, and $c = 3.300$ nm, similar to the one previously reported by others. This transformation is dependent upon the annealing temperature and time and is irreversible. Twin crystals in cell II have also been found with a (210)–(2$\bar{1}$0) boundary.

Acknowledgment. This work was supported by S.Z.D.C.'s Presidential Young Investigator Award from the National Science Foundation (DMR-9175538) and an industrial matching funding from DuPont Co.

Note Added in Proof: Very recently, through a private conversation with Professor D. C. Martin at the University of Michigan, he and his student J. Ojeda also found the diffraction patterns which show spacings generally consistent with our observations when the annealing temperature is slightly lower than normal (280 °C). In their study, poly(amic acid) precursors of PMDA–ODA were used to form droplets, and the polyimide was obtained by a thermal imidization process. This further indicates that the cell I crystal structure in PMDA–ODA is, indeed, independent of the preparing methods of this polyimide.

References and Notes

(1) Staudinger, H.; Singer, R. *Z. Kristallogr.* **1929**, *70*, 193.
(2) Geil, P. H. *Polymer Single Crystals*; Wiley-Interscience: New York, 1963; Figure VIII-3.
(3) Wunderlich, B. *Adv. Polym. Sci.* **1968**, *5*, 568.
(4) For a review, see, for example: Wunderlich, B. *Macromolecular Physics, Vol. 2, Crystal Nucleation, Growth, Annealing*; Academic: New York, 1976.
(5) Liu, J.; Rybnikar, F.; Geil, P. H. *J. Polym. Sci., Polym. Phys.* **1992**, *13*, 1467.
(6) Liu, J.; Rybnikar, F.; Geil, P. H. *J. Macromol. Sci., Polym. Phys.* **1993**, *B32* (4), 395.
(7) Harris, F. W. in *Polyimides*; Wilson, D.; Stenzenberger, H. D.; Hergenrother, Eds.; Chapman & Hall: New York, 1990, Chapter 1.
(8) Lee, H.; Stoffey, D.; Neville, K. *New Linear Polymers*; McGraw-Hill: New York, 1967; pp 183 and 224.
(9) Sroog, C. E. *J. Polym. Sci., Macromol. Rev.* **1976**, *11*, 161.
(10) Kazaryan, L. G.; Tsvankin, D. Ya.; Ginsburg, B. M.; Tuichiev, Sh.; Korhavin, L. N.; Frenkel, S. Ya. *Vysokomol. Soedin., Ser. A* **1972**, *14*, 1199.
(11) Sidorovich, A. V.; Baklagina, Yu, G.; Kenarov, A. V.; Nadezhin, Yu. S.; Adrova, N. A.; Florinskii, F. S. *J. Polym. Sci., Polym. Symp.* **1977**, *58*, 359.
(12) Conte, G.; Iliaro, L.; Patel, N. V.; Giglio, E. *J. Polym. Sci., Polym. Phys. Ed.* **1976**, *14*, 1553.
(13) Private communications. See also: Freilich, S. C.; Gardner, K. H. In *Polyimides: Materials, Chemistry and Characterization*; Feger, C., Khojasteh, M. M., McGrath, J. E., Eds.; Elsevier: Amsterdam, The Netherlands, 1989; p 520.
(14) Ojeda, J.; Martin, D. *Macromolecules* **1993**, *26*, 6557.
(15) Poon, T. W.; Saraf, R. F.; Silverman, B. D. *Macromolecules* **1993**, *26*, 3369.
(16) Tsuji, M.; Roy, S. K.; Manley, R. St. J. *J. Polym. Sci., Polym. Phys. Ed.* **1985**, *23*, 1127.
(17) Bessonov, M. I.; Koton, M. M.; Kudryavtsev, V. V. In *Polyimides, Thermally Stable Polymers*, 2nd ed.; Plenum: New York, 1987; p 250.
(18) Liu, J. Ph.D. Dissertation, Department of Polymer Science, The University of Akron, OH, 1994.
(19) Ikeda, R. M. *J. Polym. Sci., Polym. Lett.* **1966**, *4*, 35.